



Hybrid FSO–THz Technologies for 6G Access Networks: A Cost-Availability Trade-off Analysis

Downloaded from: <https://research.chalmers.se>, 2026-04-14 13:17 UTC

Citation for the original published paper (version of record):

Pendem, S., Natalino Da Silva, C., Monti, P. et al (2025). Hybrid FSO–THz Technologies for 6G Access Networks: A Cost-Availability Trade-off Analysis. International Conference on Transparent Optical Networks. <http://dx.doi.org/10.1109/ICTON67126.2025.11125338>

N.B. When citing this work, cite the original published paper.

© 2025 IEEE. Personal use of this material is permitted. Permission from IEEE must be obtained for all other uses, in any current or future media, including reprinting/republishing this material for advertising or promotional purposes, or reuse of any copyrighted component of this work in other works.

Hybrid FSO–THz Technologies for 6G Access Networks: A Cost-Availability Trade-off Analysis

Sai Vikranth Pendem*, Carlos Natalino*, Antonio Napoli†, Paolo Monti*

*Department of Electrical Engineering, Chalmers University of Technology, Gothenburg, Sweden
{vikranth, carlos.natalino, mpaolo}@chalmers.se

† Nokia, Munich, Germany {antonio.napoli@nokia.com}

Abstract—Free space optics (FSO) and terahertz (THz) communication are emerging as promising wireless technologies to meet the high data rate and low-latency requirements of 6G access networks. However, assessing their techno-economic feasibility is essential before widespread deployment. This paper analyzes the cost and availability trade-offs of hybrid FSO–THz deployments in mobile access networks, considering multiple topologies and geographic scenarios. It also evaluates their use as protection mechanisms under network failure conditions. The findings provide practical guidance on target cost and performance thresholds, helping equipment vendors and operators design resilient and cost-effective 6G access solutions.

Index Terms—6G, THz communication, Free space optics, Mobile fronthaul, Optical transport architectures, Point-to-Multipoint, CapEx, Availability.

I. INTRODUCTION

As the rollout of 5G rapidly progresses, research has intensified in recent years to enable the sixth generation (6G) of mobile communication. The ITU recommendations for IMT-2030 and beyond include high-resolution and interactive video experiences, intelligent networks, digital twins, tele-diagnostics, and many other data-hungry and latency-constrained applications [1]. To enable them, a 6G communication infrastructure should be capable of handling a peak data rate of at least 1 Tbps, a user-experienced data rate of 1 Gbps with availability of nine-nines and latency of <1 msec [2]. Optical fiber can support extremely high data traffic demands with excellent reliability. However, its deployment remains expensive, especially in difficult terrains, making it challenging and less attractive for operators to deploy fiber resources everywhere.

Consequently, alternative technologies that offer fiber-like performance without equivalent deployment costs are actively being investigated. Among these, free space optics (FSO) and terahertz (THz) communications stand out for their ability to support higher data rates than microwave and millimeter-wave links thanks to their use of higher carrier frequencies. However, FSO links are susceptible to low-visibility conditions (e.g., fog, ambient light, and atmospheric turbulence) and require precise alignment due to their strict line-of-sight nature [3]. In contrast, THz links are significantly affected by rain but require less stringent pointing accuracy [4]. Therefore, a hybrid FSO-THz communication system can address the

complementary limitations of each technology, potentially offering enhanced reliability as an alternative to fiber-based mobile transport.

The ECO-eNET project, part of Horizon Europe Smart Networks and Services Joint Undertaking, focuses on developing hybrid FSO-THz technologies, key enablers for meeting 6G requirements [5]. It aims to enable on-demand connectivity in the access segment by dynamically allocating network resources and combining fiber with FSO-THz technologies to enhance performance and efficiency. The project also addresses the control and management strategies necessary to operate them. However, there is little clarity on potential cost and availability parameters that these FSO-THz transceivers must meet for practical applications.

This paper aims to bridge this gap by analyzing the cost and reliability performance of FSO-THz technologies. This is essential in understanding under which conditions they might be viable in real-world deployments. To the best of our knowledge, this is the first study that uses a practical setting. Our analysis is based on the access segment of a mobile network deployed by a South American operator where different geotypes (dense-urban & suburban) are considered. In addition to baseline deployment cost comparisons, we also explore the potential of FSO–THz links to serve as backup under single failure scenarios. These findings offer concrete insights on the economic feasibility and performance benchmarks necessary for adopting FSO-THz solutions in next-generation mobile transport networks.

II. SYSTEM ARCHITECTURE AND DEPLOYMENT SCENARIOS

The mobile transport network considered in this study consists of three main segments: aggregation, pre-aggregation, and access, as depicted in Figure 1. The pre-aggregation segment comprises passive distribution nodes (PDNs) arranged in rings, connecting the core network via metro aggregation (MA) nodes to the access segment through fiber aggregation (FA) nodes. MA and FA nodes house optical equipment and layer-three processing capabilities, with data centers (DCs) optionally located at either. In contrast, PDNs only contain passive components for interconnecting FA nodes. In the access segment, FA nodes connect to macrocells (MCs) and/or

small cells (SCs) via fiber links. A more detailed description of the network architecture is provided in [6].

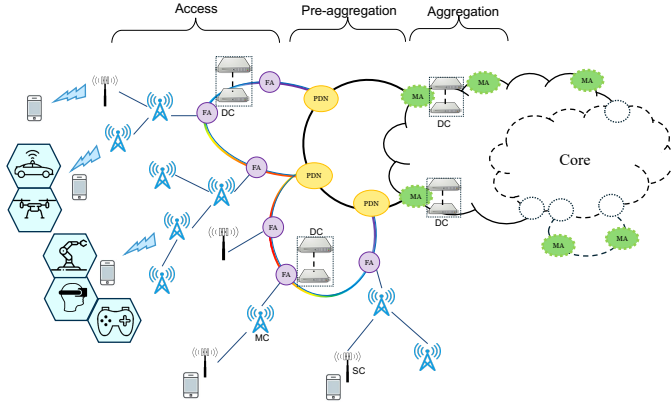


Fig. 1: Mobile transport network architecture comprising access, pre-aggregation, and aggregation segments. Small cells (SCs) and macro cells (MCs) are connected to fiber aggregation (FA) nodes through optical fiber links.

Our analysis focuses on the access segment, where the potential of a hybrid FSO–THz technology is evaluated from both cost and reliability perspectives. We consider two topology options for the access segment architecture: point-to-point (P2P) and point-to-multipoint (P2MP). We evaluate multiple deployment scenarios for each topology in which the number of hybrid FSO-THz links is varied, as discussed below. This analysis helps quantify the impact of different proportions of FSO-THz wireless equipment on the deployment cost and availability performance within a given topology.

Figure 2 (a) shows an *All-Fiber (AF) P2P* scenario, where all cell sites are connected to the FA node through optical fiber links using gray transceivers. Networking devices (NDs), placed at first-hop sites, aggregate traffic from second-hop base stations and forward it to the FA node. Figure 2 (b) illustrates an alternative P2P scenario, referred to as *SC-Wireless (SC-WL)*, in which all fiber-based SC links are replaced with hybrid FSO-THz equipment. Figure 2 (c) presents an *AF P2MP* scenario, which employs power splitters and multiplexers (MUXs) to connect MCs/SCs to the FA node via optical fiber. Since the power splitter distributes the input signal independently of wavelength, colored transceivers enable wavelength-dependent selectivity at the receiver. Figure 2 (d) depicts a *SC-WL P2MP* scenario, where fiber-based SC links are replaced with FSO-THz wireless equipment. The study also considers two additional scenarios for both P2P and P2MP topologies. Due to space constraints, these are not shown in Figure 2 but can be easily derived from the illustrated cases. The scenarios are referred to as *2-Hop-Wireless (2H-WL)* and *All-Wireless (WL)*. In the 2H-WL scenario, all second-hop links, along with SC links, are replaced by FSO–THz equipment. In the WL scenario, all links in the topology, except those at 0-hop sites, are replaced with wireless equipment, increasing the overall reliance on FSO–THz technology across cell sites. All scenarios assume a low-layer functional split (Option 7.2x

[7]), where the low PHY is processed at the base station, while the high PHY is processed at DCs located at the FA nodes.

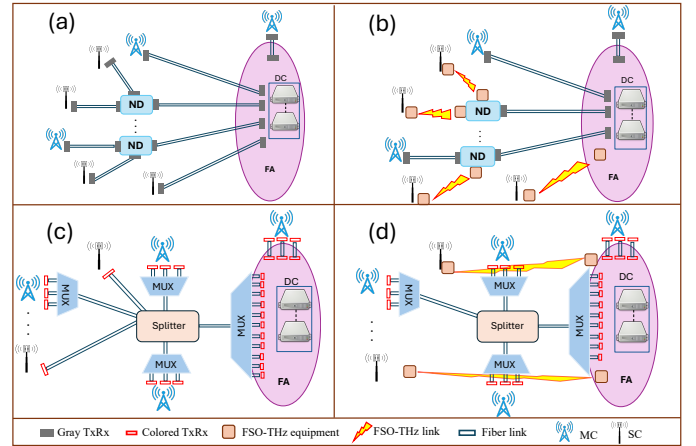


Fig. 2: Topologies considered in the study. (a) and (c) show an All-Fiber (AF) scenario for point-to-point (P2P) and point-to-multipoint (P2MP) configurations, respectively. (b) and (d) illustrate a SC-Wireless (SC-WL) scenario, where small cell (SC) links are replaced with hybrid FSO–THz equipment.

To assess the potential benefits of FSO-THz links for cost-effective failure recovery, the study assumes a single failure scenario (i.e., at most one network element—transceiver, fiber link, or network device—can fail at any given time). Three protection schemes (see Fig. 3) are considered under this assumption. The first one offers *Transceiver & ND protection* (TRx & ND protection). Specifically, each transceiver and ND is duplicated to provide backup in case of failure. However, this scheme does not protect against fiber cut (Fig. 3(a)). The second one offers *Transceiver, ND, and Fiber protection* (TRx, ND & fiber protection). This approach adds fiber redundancy to the previous scheme by duplicating each fiber link, ensuring recovery from any possible single failure (Fig. 3(b)). The third option offers *Wireless* protection. This scheme leverages the beam-steering capability of the FSO-THz equipment to dynamically re-establish connectivity when a fiber link or component fails. Consequently, it is sufficient to equip the FA node with as much wireless equipment as the maximum number of MCs or SCs that could lose connectivity under the single failure scenario assumption.

Figure 3 (c) shows how wireless protection works. If link-2 or link-3 fails, wireless transceivers W1 & W2 can restore connectivity to the affected cell sites via alternate paths using (W6,W7) or (W4,W5). If the ND connecting link-6&5 to link-3 fails, W1 and W2 can re-establish connectivity to the base stations through W5 and W4. In cases where a link is directly connected to a cell site without ND, only one wireless transceiver at the FA node is required to restore the connection in case of a link or component failure. For example, if any network element along link-1 fails, W1 or W2 can re-establish connectivity to the base station using W8. Compared to the other protection schemes, wireless protection offers

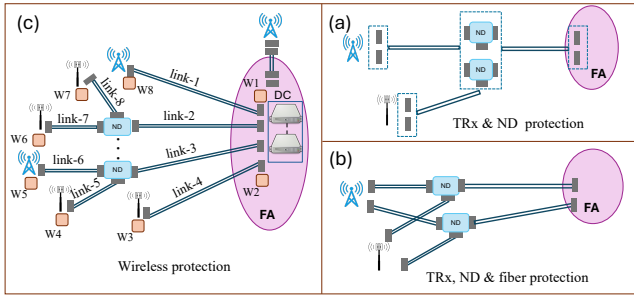


Fig. 3: Protection schemes under a single failure scenario: (a) TRx & ND protection, (b) TRx, ND & fiber protection, and (c) Wireless protection using beam-steerable FSO-THz transceivers for dynamic link reconfiguration.

enhanced resiliency with minimal redundancy, owing to the dynamic reconfiguration capabilities of beam-steerable FSO-THz transceivers.

III. CAPEX AND AVAILABILITY MODELING

This section presents the capital expenditure (CapEx) and the availability models used to evaluate the performance of the architecture/topologies described in the previous section. The CapEx value (expressed in cost units (CU)) is computed as follows:

$$\text{CapEx} = A_{c_{\text{opt}}} + A_{c_{\text{fib}}} + A_{c_{\text{wir}}} + \text{Comp}. \quad (1)$$

$A_{c_{\text{opt}}}$ is the cost of the optical equipment, including transceivers, splitters, optical multiplexers, and NDs. $A_{c_{\text{fib}}}$ represents the cost of deploying the fiber infrastructure, including trenching. $A_{c_{\text{wir}}}$ denotes the total cost of the FSO-THz transceivers. The term Comp represents the cost of the computing resources required at the cell sites and the DCs at FA nodes for baseband processing.

The cost of a hybrid FSO-THz wireless transceiver (C_{wir}) is computed using the linear cost model defined as:

$$C_{\text{wir}} = \alpha \times C_{10G}, \quad (2)$$

where α is a scaling parameter, and C_{10G} represents the cost of a 10 Gbps gray optical transceiver, expressed in CU.

To compute the availability of a connection between an FA node and a cell site, we account for the mean-time-to-failure (MTTF) and mean-time-to-repair (MTTR) values of all the components along the path. This includes transceivers, multiplexers, splitters, fiber segments, and NDs. The availability of a link is calculated as $A_{\text{link}} = 1 - UA_{\text{link}}$, where UA_{link} represents the overall unavailability computed as the sum of the individual unavailabilities of all components present along the link, assuming no protection is in place.

The unavailability of an individual component is given by:

$$UA_{\text{device}} = \frac{\text{MTTR}_{\text{device}}}{\text{MTTF}_{\text{device}} + \text{MTTR}_{\text{device}}} \quad (3)$$

To calculate the percentage of cell sites with availability greater than a specific threshold, we define a parameter called percentage availability, expressed as :

$$P(A) = \frac{\text{sites with } A > A_{\text{thres}}}{\text{total sites}} \times 100(\%). \quad (4)$$

IV. PERFORMANCE EVALUATION AND TRADE-OFF ANALYSIS

This section presents the cost vs. availability performance of the deployment scenarios mentioned in Sec. II. Two geo-types are considered, i.e., dense-urban and suburban. These represent two extremes in network topology characteristics, including cell site density (MCs and SCs), average link distances, and cell site capacity. The number of MCs and SCs at different hops, the number of FA nodes, the distances between them and the traffic requirements are taken from Table 2 in [6]. The total traffic across the network amounts to 29.3 Tbps and 66.4 Tbps for the suburban and dense-urban case, respectively. This difference is due to the higher cell site density and shorter hop lengths in the dense-urban scenario compared to the suburban one.

For the P2P topology, we employ 25 Gbps and 100 Gbps gray transceivers. For the P2MP topology, we use 25 Gbps colored ones. The hybrid FSO-THz transceivers are assumed to support adaptive bit rate, up to 100 Gbps. Their cost is modeled as described in Eq. (2). The cost and the MTTF values of all the network elements used in the performance assessment work are from Table 3 in [6]. Results are obtained through simulations using custom Python scripts that emulate the network deployment.

Figure 4 shows how CapEx varies with the scaling factor α for the P2P topology in suburban and dense-urban environments. The value of α at which each wireless scenario (SC-WL, 2H-WL, WL) reaches cost parity with AF deployment increases as more cell sites are replaced with wireless links. This trend reflects the steeper slope and lower intercept in CapEx curves for wireless-heavy configurations, indicating a lower initial cost but greater sensitivity to the unit cost of hybrid FSO-THz transceivers. In dense-urban scenarios, where the number of cell sites is higher than in suburban areas, the SC-WL configuration reaches cost parity with AF at approximately $\alpha \approx 180$. This implies that, across both geo-types, the cost scaling parameter α should remain below 180 for any wireless deployment scenario to achieve a non-zero CapEx gain over AF. For the P2MP topology, the α threshold at which SC-WL achieves cost parity is even higher (figure omitted due to space constraints), indicating that the most stringent cost condition is governed by the P2P topology. Therefore, the subsequent analysis focuses on P2P deployments for both geo-types.

Table I summarizes the CapEx gains achievable with the SC-WL configuration vs. the AF scenario for two different α values. Results show that the CapEx gains in the dense-urban case are more sensitive to α than the suburban geo-type, primarily due to the higher number of SC links in dense-urban deployments.

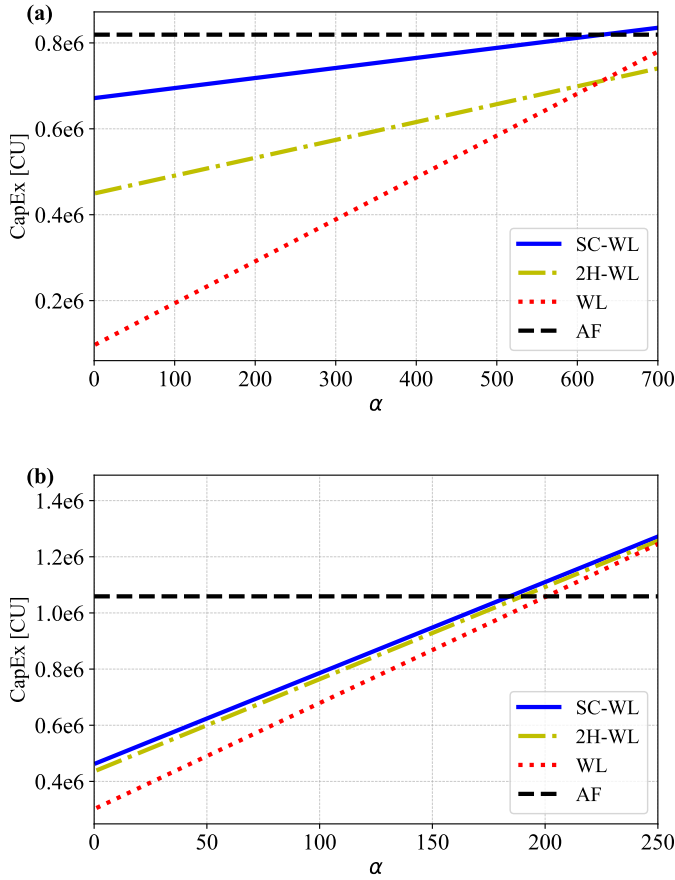


Fig. 4: CapEx variation as a function of the cost scaling factor (α) for different wireless deployment scenarios with a P2P topology. (a) Suburban and (b) dense-urban areas.

TABLE I: CapEx comparison between SC-WL and AF scenarios in the P2MP topology for different values of the cost scaling factor α across suburban and dense-urban geo-types.

Geo-type	α	AF [CU]	SC-WL [CU]	Gain (%)
Suburban	100	896,922	766,377	14.5%
Suburban	180	896,922	785,097	12.5%
Dense-urban	100	1,209,430	847,530	29.9%
Dense-urban	180	1,209,430	1,104,730	8.7%

Figure 5 presents the cost breakdown for all deployment scenarios for P2P topologies in dense and suburban environments. The breakdown reflects the cost components defined in Eq. (1) evaluated for $\alpha = 100$ and $\alpha = 180$, alongside the AF baseline. The cost of computing resources remains constant as it depends solely on the total number of cell sites and the assumed functional split. In the AF scenario, the total CapEx is dominated by $A_{c_{\text{fib}}}$ driven by fiber deployment costs. The figure illustrates the CapEx advantages of introducing wireless links. As the number of wireless links increases, the cost associated with fiber deployment decreases. This highlights the cost-saving potential of wireless deployments, especially in areas where fiber installation is challenging or expensive. The

$A_{c_{\text{opt}}}$ component remains non-zero even in the WL scenario. This is because 0-hop links, which connect cell sites located at the FA node, are always assumed to be served by fiber in this study.

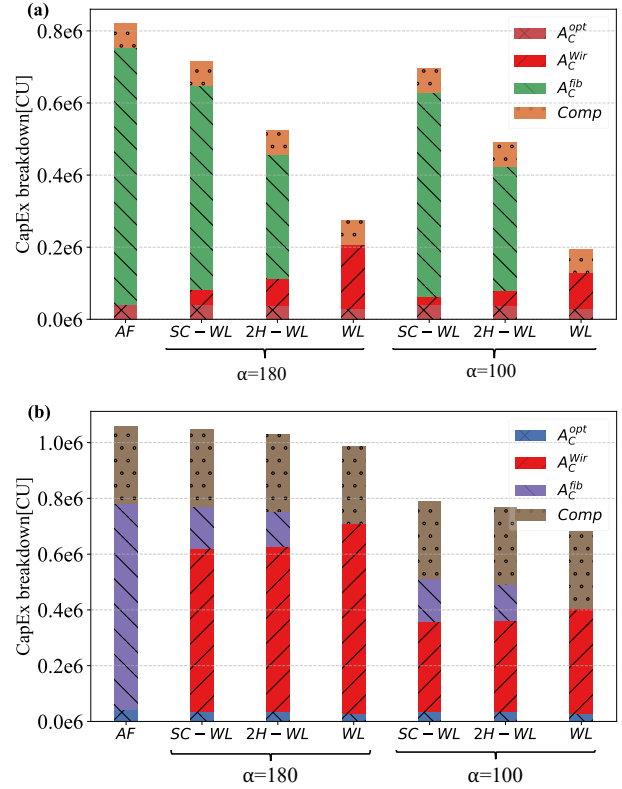


Fig. 5: CapEx breakdown for all P2P deployment scenarios in (a) suburban and (b) dense-urban geo-types.

Figure 6 shows how CapEx varies with α for the different protection options described in Sec. II. Results indicate values up to 180 provide non-zero CapEx gains. This is because the level of resiliency offered by wireless protection is comparable to that of the TRx, ND & fiber protection scheme in the event of a single link or node failure, while avoiding the cost of duplicating the fiber resources and optical transceivers.

Figure 7 shows the percentage of cell sites that achieve different availability thresholds under various deployment scenarios. A constant MTTR of 4 hours is assumed for all the devices. For the hybrid FSO-THz equipment, an MTTF of 25 years is used, corresponding to the highest MTTF value reported for microwave equipment in Table 3 of [6]. The AF scenario achieves higher or equal availability levels than any wireless configurations across all thresholds. In all wireless scenarios, 100% of cell sites reach an availability above 0.99990 under the assumed MTTF value, with a subset achieving values exceeding 0.99998. However, as the proportion of wireless links increases, the percentage of sites meeting the highest availability thresholds decreases. These findings highlight a fundamental trade-off in 6G network design. While the hybrid FSO-THz solutions offer high data rates and poten-

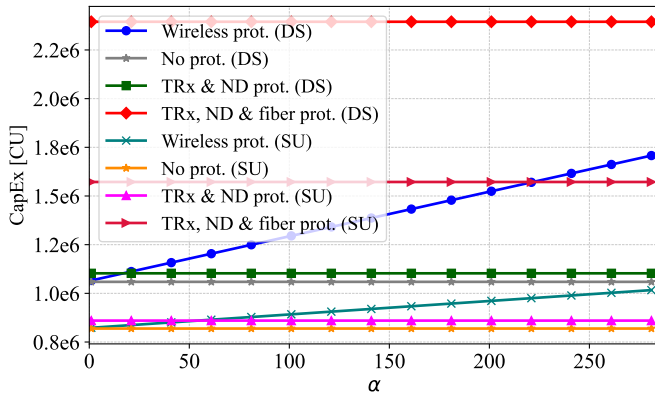


Fig. 6: CapEx as a function of α for different protection schemes for the suburban (SU) and dense-urban (DU) geo-types.

tial cost advantages, their practical deployment requires high-quality, reliable hardware to achieve ultra-high availability levels traditionally associated with fiber-based systems.

V. CONCLUSION

This work provides key insights into the cost thresholds and deployment feasibility of hybrid FSO-THz wireless transceivers for 6G mobile communication networks. We analyzed CapEx and availability variations resulting from using different proportions of FSO-THz equipment in a real-world network deployment, considering P2P and P2MP topologies across two geo-types: dense-urban and suburban. In addition, we evaluated the potential of using hybrid FSO-THz transceivers as an alternative to traditional transceivers and fiber duplication for protection against single failures. The results indicate that, for the deployment scenarios considered in this study, the α must remain below 180 for hybrid FSO-THz deployments to yield CapEx savings relative to the AF baseline. While this threshold is specific to the case analyzed, it provides a useful estimate of the cost conditions under which these technologies become economically viable. The findings offer practical design guidelines for equipment vendors and network operators aiming to deploy cost-effective and resilient 6G access networks using hybrid FSO-THz links, either alongside or in place of fiber.

ACKNOWLEDGMENT

This work has been partially supported by the European Union's Horizon 2022 - MSCA project EMPOWER-6G (101120332) and by the European Union's Horizon Europe research and innovation program through the ECO-eNET project (10113933).

REFERENCES

[1] M. Series, "Imt vision - framework and overall objectives of the future development of imt for 2020 and beyond," *Recommendation ITU*, vol. 2083, no. 0, pp. 1–21, 2015.

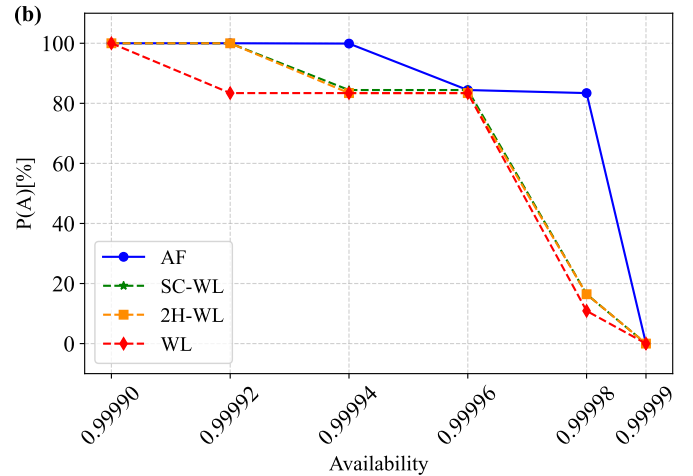
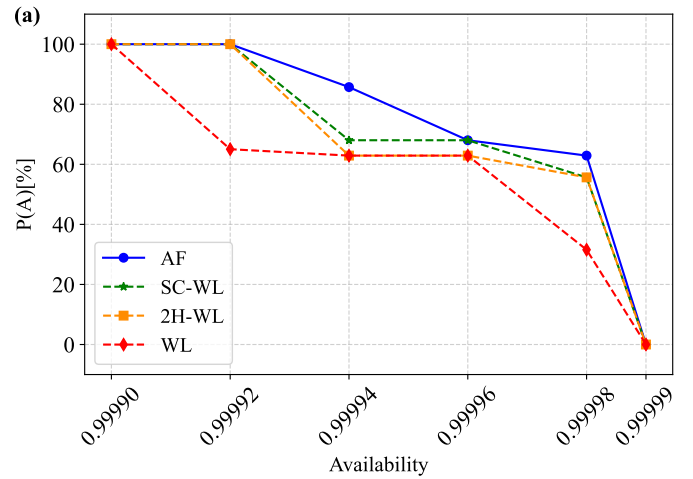


Fig. 7: Availability distribution of P2P deployment scenarios across different thresholds. (a) Suburban and (b) dense-urban geo-types.

[2] C.-X. Wang, X. You, X. Gao, X. Zhu, Z. Li, C. Zhang, H. Wang, Y. Huang, Y. Chen, H. Haas, J. S. Thompson, E. G. Larsson, M. D. Renzo, W. Tong, P. Zhu, X. Shen, H. V. Poor, and L. Hanzo, "On the road to 6G: Visions, requirements, key technologies, and testbeds," *IEEE Communications Surveys & Tutorials*, vol. 25, no. 2, pp. 905–974, 2023.

[3] H. Kaushal, V. K. Jain, and S. Kar, *Free Space Optical Communication*, B. Mukherjee, Ed. New Delhi: Springer, 2017.

[4] P. K. Singya, B. Makki, A. D'Errico, and M.-S. Alouini, "Hybrid fso/thz-based backhaul network for mmwave terrestrial communication," *IEEE Transactions on Wireless Communications*, vol. 22, no. 7, pp. 4342–4359, 2023.

[5] R. Raj, D. Dass, K. Kaeval, S. Patri, V. Sleiffer, B. Baeuerle, W. Heni, M. Ruffini, C. Browning, A. Naughton *et al.*, "Towards efficient confluent edge networks," in *2024 Joint European Conference on Networks and Communications & 6G Summit (EuCNC/6G Summit)*. IEEE, 2024, pp. 1163–1168.

[6] M. Lashgari, F. Tonini, M. Capacchione, L. Wosinska, G. Rigamonti, and P. Monti, "Techno-economics of fiber versus microwave for mobile transport network deployments," *Journal of Optical Communications and Networking*, vol. 15, no. 7, pp. C74–C87, 2023.

[7] "O-ran fronthaul working group: Control, user and synchronization plane specification v7.02," O-RAN Alliance, Tech. Rep., 2022, <https://www.o-ran.org/specifications>.